Cell Reports

Stem-Cell-like Properties and Epithelial Plasticity Arise as Stable Traits after Transient Twist1 Activation

Graphical Abstract
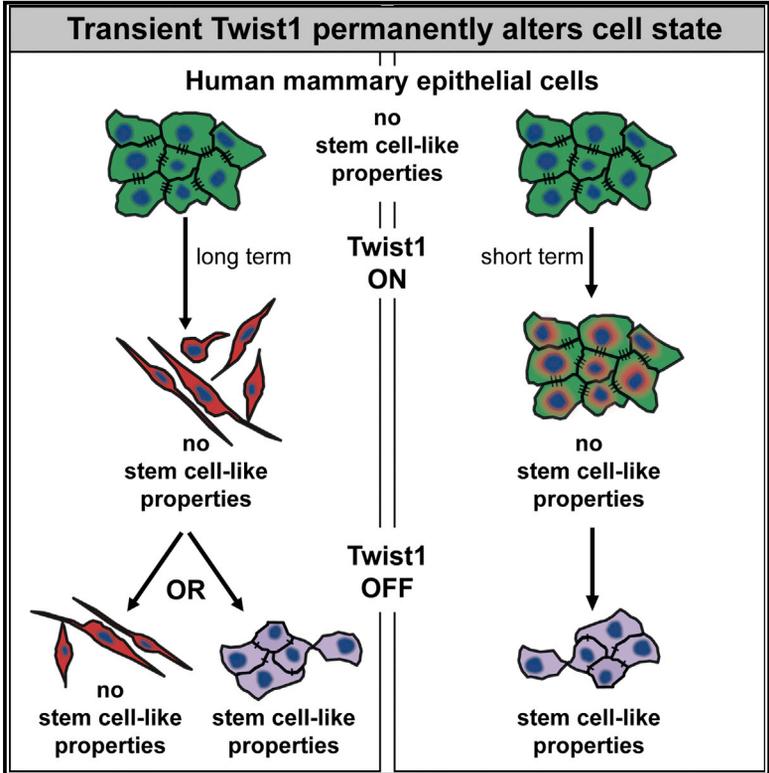
Authors

Johanna M. Schmidt, Elena Panzilius, ..., Karl Sotlar, Christina H. Scheel

Correspondence

christina.scheel@helmholtz-muenchen.de

In Brief

Schmidt et al. show that Twist1, a master regulator of the epithelial-mesenchymal transition, primes mammary epithelial cells for stem-cell-like properties. Following transient Twist1 activation, cells display an altered, epithelial cell state characterized by invasive growth, plasticity, and a unique gene expression profile.

Highlights

- Transient Twist1 activation primes cells for stem-cell-like traits

- Stable stem-cell-like traits arise after Twist1 deactivation

- Transient, not continuous, Twist1 activity promotes invasive growth

- Transient Twist1 elicits a stably altered plastic epithelial cell state

Report

Stem-Cell-like Properties and Epithelial Plasticity Arise as Stable Traits after Transient Twist1 Activation

Johanna M. Schmidt,[1] Elena Panzilius,[1] Harald S. Bartsch,[2] Martin Irmler,[3] Johannes Beckers,[3,8] Vijayalakshmi Kari,[4] Jelena R. Linnemann,[1] Diana Dragoi,[1] Benjamin Hirschi,[1] Uwe J. Kloos,[1] Steffen Sass,[5] Fabian Theis,[5,6] Steffen Kahlert,[7] Steven A. Johnsen,[4] Karl Sotlar,[2] and Christina H. Scheel[1,*]

[1]Institute of Stem Cell Research, Helmholtz Center for Health and Environmental Research Munich, 85764 Neuherberg, Germany
[2]Institute of Pathology, Medical School, Ludwig Maximilian University, 80337 Munich, Germany
[3]Institute of Experimental Genetics, Helmholtz Center Munich, 85764 Neuherberg, Germany
[4]Department of General, Visceral and Pediatric Surgery, University Medical Center, 37075 Göttingen, Germany
[5]Institute of Computational Biology, Helmholtz Center Munich, 85764 Neuherberg, Germany
[6]Department of Mathematics, Technical University Munich, 85747 Garching, Germany
[7]Department of Obstetrics and Gynecology, Medical School, Ludwig Maximilian University, 80337 Munich, Germany
[8]Department of Experimental Genetics, Technical University Munich, 85354 Freising, Germany
*Correspondence: christina.scheel@helmholtz-muenchen.de
http://dx.doi.org/10.1016/j.celrep.2014.12.032

SUMMARY

Master regulators of the epithelial-mesenchymal transition such as Twist1 and Snail1 have been implicated in invasiveness and the generation of cancer stem cells, but their persistent activity inhibits stem-cell-like properties and the outgrowth of disseminated cancer cells into macroscopic metastases. Here, we show that Twist1 activation primes a subset of mammary epithelial cells for stem-cell-like properties, which only emerge and stably persist following Twist1 deactivation. Consequently, when cells undergo a mesenchymal-epithelial transition (MET), they do not return to their original epithelial cell state, evidenced by acquisition of invasive growth behavior and a distinct gene expression profile. These data provide an explanation for how transient Twist1 activation may promote all steps of the metastatic cascade; i.e., invasion, dissemination, and metastatic outgrowth at distant sites.

INTRODUCTION

During epithelial-mesenchymal transition (EMT), apical-basal polarized epithelial cells are converted to front-to-back polarized mesenchymal cells with unrestricted motility (Lamouille et al., 2014). EMT programs effect morphogenetic steps during embryogenesis and are orchestrated by pleiotropic transcription factors (TFs) such as Twist1 and Snail1 (Lim and Thiery, 2012; Nieto, 2011).

EMTs have been implicated in metastatic dissemination of carcinoma cells and in the generation of cancer stem cells (CSCs; Ansieau, 2013; Lamouille et al., 2014; Scheel and Wein-

berg, 2012). However, metastases of breast cancer are typically epithelial (Kowalski et al., 2003), and numerous experimental systems have shown that mesenchymal-epithelial transition (MET) is required for actively proliferating metastases (Chaffer et al., 2006; Ocaña et al., 2012; Stankic et al., 2013; Tran et al., 2014; Tsai et al., 2012). Other studies indicate that epithelial, rather than mesenchymal, attributes are enriched in tumorigenic cell populations, leading to the conclusion that EMT inhibits stem-cell-like properties (Celià-Terrassa et al., 2012; Korpal et al., 2011; Sarrio et al., 2012). To reconcile these contrasting observations, we closely monitored the dynamics and functional consequences of transient Twist1 activation in human mammary epithelial cells (HMLEs). Thereby, we discovered that Twist1 primes a subset of cells for stem-cell-like traits that emerge as stable traits after Twist1 deactivation.

RESULTS

EMT and Stem-Cell-like Traits Induced by Transient Twist1 Activation

We utilized immortalized HMLEs (Elenbaas et al., 2001) retrovirally transduced with Twist1 fused to a mutated estrogen receptor (ER) ligand binding domain (Casas et al., 2011). To prevent selection of pre-existing mesenchymal cells (Scheel et al., 2011), we sorted bulk HMLE cells into purified epithelial subpopulations with high or low levels of the surface marker CD24 (24^{hi} and 24^{lo}; Figures 1A–1C).

First, Twist1 was activated for 15 days by adding 4-hydroxytamoxifen (TAM) to the growth medium every 2 days. During this period, EMT manifested as a progressive loss of E-cadherin expression, upregulation of vimentin, and acquisition of front-to-back polarization (Figures 1D and S1A). After TAM withdrawal, some 24^{hi} cells reverted back to an epithelial phenotype, indicated by re-expression of E-cadherin, whereas others remained mesenchymal (Figures 1D and S1A). E-cadherin upregulation as

Figure 1. EMT and Stem-Cell-like Traits Induced by Transient Twist1 Activation

(A) Fluorescence-activated cell sorting (FACS): CD44 and CD24 cell surface staining of HMLE-Twist1-ER cells and postsort analysis after 3 days in culture.

(B) Histogram overlay of postsort analysis 24^{hi} (gray) and 24^{lo} (blue).

(C) Bright-field microscopy: 24^{neg} cells display a mesenchymal morphology, whereas 24^{lo} and 24^{hi} cells are epithelial. Scale bar represents 100 μm.

(legend continued on next page)

well as downregulation of several mesenchymal markers at the transcriptional level also suggested MET in a subset of 24^{hi} cells (Figure S1B). Twist1 deactivation after TAM withdrawal was confirmed by monitoring mRNA levels of Wnt5a, a transcriptional Twist1 target (Shi et al., 2014). Strikingly, none of the 24^{lo} cells re-expressed E-cadherin (Figures 1D and S1A). These responses could not be attributed to different Twist1 levels since immuno-fluorescence staining of 24^{hi} and 24^{lo} cells revealed similarly heterogeneous expression before, during, and after TAM treatment (Figures S1C and S1D).

To test motility, we assessed the ability of single cells to migrate through porous membranes. As expected, migrating cells were significantly increased in mesenchymal cell populations generated by TAM treatment (Figures S1E and S1F). After TAM withdrawal, the proportion of migrating cells decreased in the 24^{hi} cells, corresponding to the reappearance in epithelial cells. To assess stem-cell-like traits, we utilized the mammo-sphere (MS) assay, which quantifies clonal growth in anchorage independence (Dontu et al., 2003). To determine MS-forming ability in 24^{hi} and 24^{lo} cells after complete EMT, cells were either continuously treated during MS formation (Twist1 on, +) or TAM was withdrawn upon plating (Twist1 on/off, +/−; Figure 1E). Unexpectedly, MS formation was only observed upon TAM withdrawal, indicating that MS formation was dependent on transient, but not continuous, Twist1 activation (Figures 1F, S1G, and S1H).

Given these results, we determined the impact of MET on MS formation by withdrawing TAM for 9 days before plating cells into the MS assay (Figure 1E). Remarkably, allowing MET to take place increased the frequency of MS-forming cells 20-fold in 24^{hi} cells (Figures 1G and S1I). Serial passaging in limiting dilution enriched the frequency of MS-forming cells to one of three cells, suggesting long-term repopulating ability (Figure 1H). Taken together, these observations indicated that Twist1 elicits a potential for MS formation in 24^{hi} HMLE cells that emerges only after Twist1 deactivation.

Stem-Cell-like Traits Are Enriched in Cells that Undergo MET

To determine whether MS-forming ability was contained within mesenchymal cells or those that underwent MET, we employed differential trypsinization to obtain fractions enriched for mesenchymal (M), epithelial (E), and strongly trypsin-resistant epithelial (E+) cells (Figures 2A and 2B). Of note, the E fraction did contain 5%–10% mesenchymal cells. Remarkably, MS-forming cells were highly enriched in the E fraction but depleted in the M fraction (Figure 2C). The E+ fraction generated few MS, suggesting that MS-forming cells display epithelial plasticity. In support of these observations, immunofluorescence staining revealed MS to contain both E-cadherin- and vimentin-positive cells (Fig-

ure 2D) and the expression of intermediate transcript levels of E-cadherin and mesenchymal markers (Figure 2E). Wnt5a levels remained low, indicating that Twist1 was not reactivated. Thus, MS-forming cells were enriched in cell populations with epithelial plasticity, but not in those with a fixed mesenchymal or epithelial phenotype.

In support of these observations, 97% of MS cells retained expression of the epithelial marker CD24 (Figures 2F and S2A). To elucidate whether CD24 levels predicted MS-forming ability, TAM-treated 24^{hi} cells were sorted into $CD24^{neg}$ and $CD24^{hi}$ populations (Figure 2G). Remarkably, MS-forming ability was enriched 6-fold in the $CD24^{hi}$ compared with the $CD24^{neg}$ population (Figure 2H). Moreover, $CD24^{hi}$ cells passed through MET, whereas $CD24^{neg}$ cells maintained a mesenchymal phenotype, indicating that MS-forming ability is enriched in cells undergoing MET after Twist1 deactivation (Figure 2I).

To determine whether passage through EMT was required to prime cells for MS-forming ability, cells were treated with TAM for 24, 48, and 72 hr followed by (1) plating into the MS assay or (2) plating after a 9-day period of TAM withdrawal (Figure S2B). During this short-term induction, cell morphology, E-cadherin and vimentin protein subcellular localization and transcript levels of epithelial and mesenchymal markers did not change significantly compared with control cells (Figures S2C and S2D). Strikingly, 48 hr of TAM-treatment followed by delayed plating was sufficient to generate MS with long-term repopulating activity (Figures S2E and S2F). These results suggest that cells primed for MS-forming ability by Twist1 expand during the period of TAM withdrawal or progressively convert to MS-forming cells. However, complete EMT did not appear to be required for Twist1 to prime epithelial cells for MS-forming ability.

MS-Forming Cells Display Invasive Growth in 3D Collagen Gels

Considering functions of Twist1 that contribute to MS formation independently of EMT, we reasoned that MS-forming cells survive anchorage independence (Frisch and Francis, 1994). Indeed, in contrast to 24^{hi} control, cells treated for 15 days with TAM survived prolonged anchorage independence and maintained this acquired trait after TAM withdrawal (Figures 3A and 3B).

Based on these observations, we tested whether the inability of cells with active Twist1 to form MS was linked to lack of proliferation in a 3D environment. Indeed, when plated as single-cell suspensions in collagen gels, cells with active Twist1 formed markedly fewer colonies than control or MS-derived cells (Figures 3C–3E). In contrast, TAM-treated cells proliferated vigorously in monolayer culture, suggesting that Twist1 activity specifically suppressed proliferation under 3D conditions (Figure 3F).

(D) Immunofluorescence: E-cadherin (green), vimentin (red), and 4′,6-diamidino-2-phenylindol-dihydrochlorid (DAPI) (blue) in FACS-purified 24^{hi} and 24^{lo} cells: control (−), treated with TAM for the indicated number of days and followed by 9 days of withdrawal. Scale bar represents 20 μm.

(E) Setup for MS assay: 24^{hi} or 24^{lo} cells with TAM for 15 days before plating. TAM was continued (+) or discontinued (+/−) or cells were cultured without TAM for 9 days prior plating (+/− 9d).

(F) Quantification of MS formed by 24^{hi} (gray) and 24^{lo} (blue) cells treated according to (E). n.d., not detectable (n = 20).

(G) Quantification of MS according to (E). n.d., not detectable (n = 20).

(H) Limiting dilution analysis: 24^{hi} cells (+/− 9 days TAM) serially passaged for four generations (n = 10 per generation).

Data are presented as mean ± SEM. See also Figure S1.
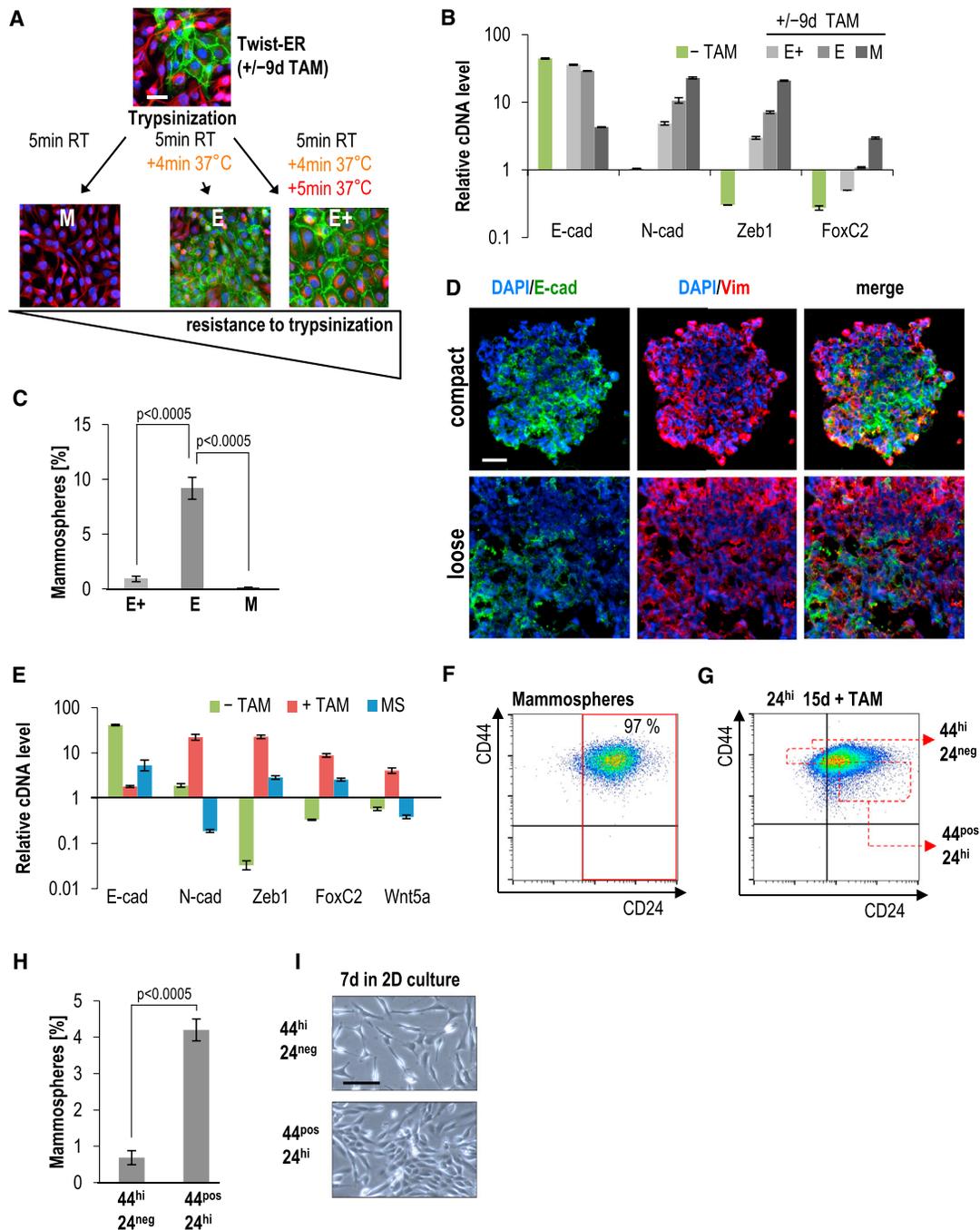
Figure 2. Stem-Cell-like Traits Are Enriched in Cells that Undergo MET

(A) Differential trypsinization: transiently TAM-treated 24^{hi} cells were separated into a mesenchymal (M), epithelial (E), and strongly trypsin-resistant epithelial (E+) fraction. Immunofluorescence: E-cadherin (green), vimentin (red), and DAPI (blue). Scale bar represents 20 μm.

(B) RT-PCR: E-cadherin, N-cadherin, Zeb1, and FoxC2 mRNA expression in 24^{hi} control (−) and in differentially trypsinized M, E, and E+ fractions (n = 3).

(C) MS assay: quantification of MS formed by M, E, and E+ fractions (n = 20).

(D) Immunofluorescence: E-cadherin (green), vimentin (red), and DAPI (blue) of compact and loose MS. Scale bar represents 100 μm.

(E) RT-PCR: E-cadherin, N-cadherin, Zeb1, FoxC2, and Wnt5a mRNA expression of 24^{hi} control (−), 15-day TAM (+) and MS (n = 3).

(F) FACS: CD44 and CD24 cell surface staining of MS.

(G) FACS: layout for resorting of 15-day TAM-treated 24^{hi} cells into a $CD44^{hi}/CD24^{neg}$ and a $CD44^{pos}/CD24^{hi}$ population.

(H) Quantification of MS formed by resorted $CD44^{hi}/CD24^{neg}$ and $CD44^{pos}/CD24^{hi}$ cells according to (G) (n = 20).

(I) Bright-field microscopy: images of resorted populations (according to G) taken 7 days after sort. Scale bar represents 50 μm.

Data are presented as mean ± SEM. See also Figure S2.
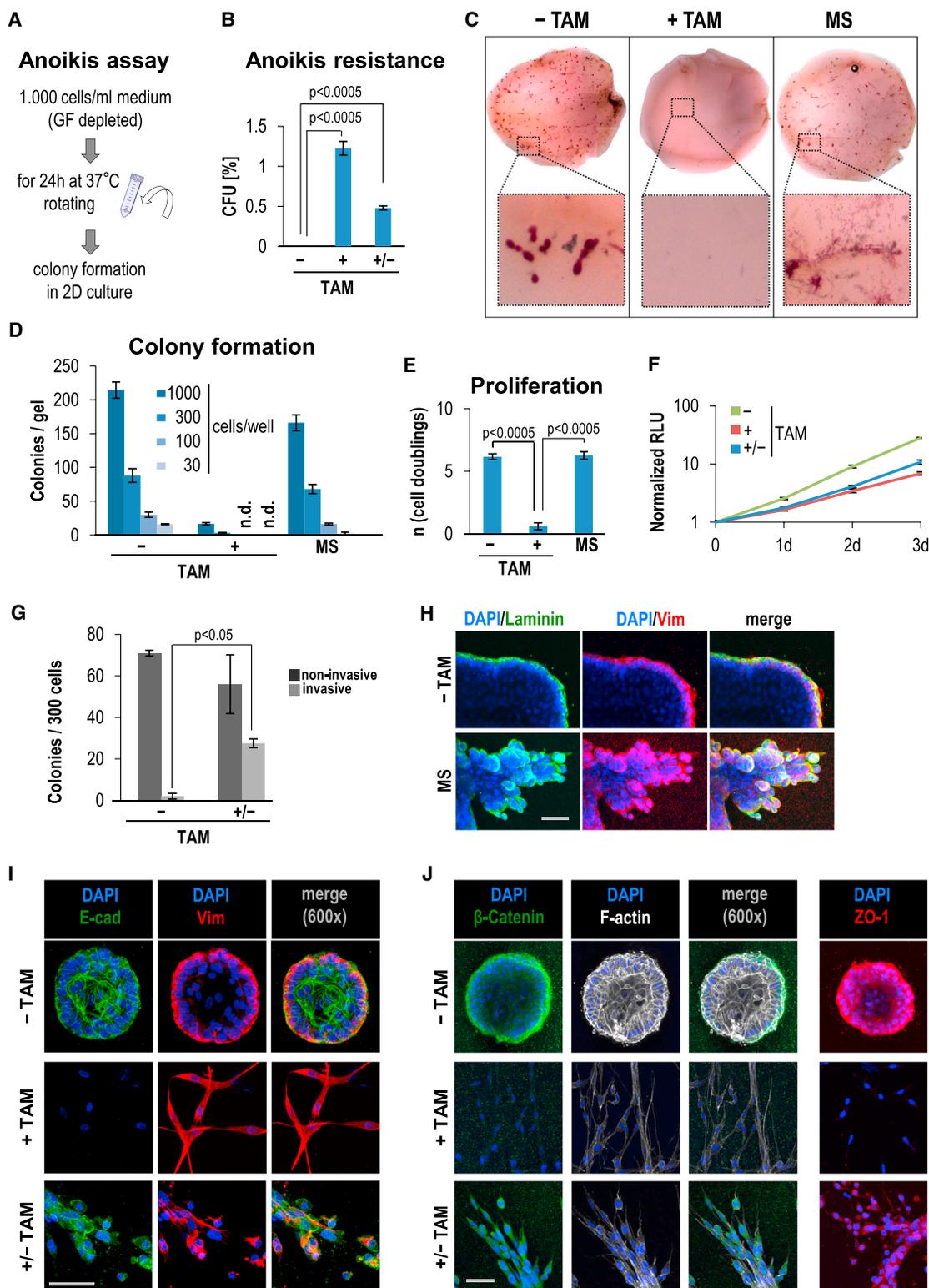
Figure 3. MS-Forming Cells Display Invasive Growth in 3D Collagen Gels

(A) Anoikis assay: experimental setup. GF, growth factor.

(B) Anoikis assay: colony-forming units (CFUs) of HMLE-Twist1-ER 24^{hi} cells in 2D after anoikis challenge: control (−), 15-day TAM (+), and 15-day TAM followed by 3-day withdrawal (+/−) prior to assay (n = 3).

(legend continued on next page)

With respect to morphology, the round colonies formed by 24^{hi} control cells displayed smooth margins with continuous laminin-1 expression (a basement membrane component; Figures 3C and 3H; Movie S1). The elongated colonies generated by MS-derived cells displayed patchy laminin-1 expression, indicating invasive growth. Consistent with a noninvasive phenotype, colonies generated by 24^{hi} control cells frequently contained a lumen and displayed a basal layer of E-cadherin/vimentin-positive cells, membranous β-catenin, and expression of the tight-junction component ZO-1 as well as cortical F-actin (Figures 3I and 3J; Movie S2). Clumps and single cells detaching from the margins were observed in colonies generated after transient Twist1 activation. Remarkably, these invading cells remained E-cadherin positive, expressed membranous β-catenin, and ZO-1 and simultaneously showed cortical F-actin as well as stress fibers. In contrast, cells with active Twist1 remained mesenchymal and were dispersed in the collagen gel as singly invading cells. Together, these results indicated that transient Twist1 activation facilitates the coexistence of epithelial and mesenchymal traits, thereby enabling invasive growth.

Transient Snail1 Activation Is Sufficient to Elicit MS-Forming Ability

Next, we determined whether other EMT-TFs might also prime cells for stem-cell-like traits and epithelial plasticity. Analogous to our strategy employed for HMLE-Twist1-ER cells (Figure 1A), we purified an epithelial CD24^{hi} population from HMLE-Snail1-ER cells (Figures S3A and S3B; Mani et al., 2008). In contrast to Twist1-ER, many epithelial cells did not convert to a mesenchymal phenotype after prolonged TAM treatment (Figures S3C and S3G). This incomplete EMT was reflected at the functional level where, in contrast to TAM-treated Twist1-ER cells, we observed a modest increase in migratory cells (Figure S3D). Moreover, MS-forming cells were generated both in continued presence and absence of TAM and preceded that of mesenchymal cells (3 days versus 6 days, respectively; Figures S3C and S3E). However, serial passaging enriched for MS-forming cells more efficiently after TAM withdrawal (Figure S3F). Therefore, Snail1 induced MS-forming potential as a stable trait that is maintained after its deactivation.

Transient Twist1 Activation Permanently Alters Cell State

Our data suggested that stem-cell-like properties and epithelial plasticity arise in some cells as stable traits after transient Twist1 or Snail1 activation. To determine whether these changes were indicative of an altered cell state, we performed gene expression profiling of HMLE subpopulations: (1) epithelial 24[lo] and 24^{hi} cells before Twist1 activation, (2) 24[lo] and 24^{hi} cells with active Twist1, (3) 24^{hi} cells after transient Twist1 activation, and (4) MS (Figure 4A). Principal component analysis following unsupervised clustering indicated distinct cell states corresponding to these subpopulations (Figure 4B). As expected, RNA expression profiles of cells after transient Twist1 activation and MS clustered in-between epithelial and mesenchymal populations (PC2). However, MS were different to all other cell states (PC1). To identify genes regulated by transient Twist1 or Snail1 activation independently of culture conditions, differentially expressed genes in MS and 2D-cultured cells after transient Twist1 activation were compared with epithelial and mesenchymal populations. Considering a concordant trend, we identified a set of 189 genes, representing the cell state arising after transient Twist1 or Snail1 activation (Figures 4C–4E). GO-term analysis revealed terms associated with intracellular protein kinase signaling to be significantly overrepresented within the 189-gene signature (Figure 4F). ROS1, an orphan receptor tyrosine kinase considered an oncogene in a subset of non-small-cell lung carcinomas (Bergethon et al., 2012), was validated by RT-PCR to be induced by Twist1 and further upregulated after Twist1 deactivation (Figure S4A). Chromatin immunoprecipitation confirmed that Twist1 directly binds the ROS1 promoter (Figure 4G). Next, we treated late-passage MS with the small-molecule Crizotinib, thereby preventing phosphorylation and signaling through ROS1 (Rossi et al., 2014). Crizotinib reduced MS formation significantly (1.5-fold at 0.3 μM; Figures 4H, S4B, and S4C). This effect was further increased upon passaging of MS, suggesting efficient inhibition of long-term repopulating ability (Figure S4D).

DISCUSSION

Following the discovery that EMT generates CSCs (Mani et al., 2008; Morel et al., 2008), efforts have focused on targeting mesenchymal cells within breast cancer cell populations (Gupta et al., 2009; Tam et al., 2013). However, our data indicate that transient Twist1 activation enabled long-term invasive growth by promoting coexistence of epithelial and mesenchymal traits, whereas constitutive Twist1 activation switched cells to a migratory, nonproliferative state. According

(C) 3D collagen gels: carmine staining of colonies formed by 24^{hi} cells: control (−TAM), 15 days TAM continued during assay (+ TAM) and MS-derived (MS) (1,000 cells per well).

(D) 3D collagen gels: quantification of colonies. Cells grown as described in (C). n.d., not detectable (n = 3).

(E) 3D collagen gels: number of population doublings. Cells were grown as described in (C) (n = 3).

(F) Growth curves: 2D proliferation of 24^{hi} cells, control (−), 15-day TAM and continued TAM every 24 hr (+) or not (+/−) for a duration of 4 days (n = 10).

(G) 3D collagen gels: Quantification of non-invasive colonies (dark gray) and invasive colonies (light gray). Assessed by staining for E-cadherin and vimentin (n = 2).

(H) Confocal microscopy of 3D collagen gels: laminin-1 (green), vimentin (red), and DAPI (blue); colonies formed by 24[hi] control (−TAM) or MS-derived cells (MS). Scale bar represents 100 μm.

(I) Confocal microscopy of 3D collagen gels: E-cadherin (green), vimentin (red), and DAPI (blue): 24[hi] control (−TAM), 16-day TAM and continued (+) or not continued (+/−). Scale bar represents 50 μm.

(J) Confocal microscopy of 3D collagen gels: β-catenin (green), F-actin (white), ZO-1 (red), and DAPI (blue): 24[hi] control (−TAM), 15d TAM and continued (+) or not continued (+/−). Scale bar represents 50 μm.

Data are presented as mean ± SEM. See also Figure S3.
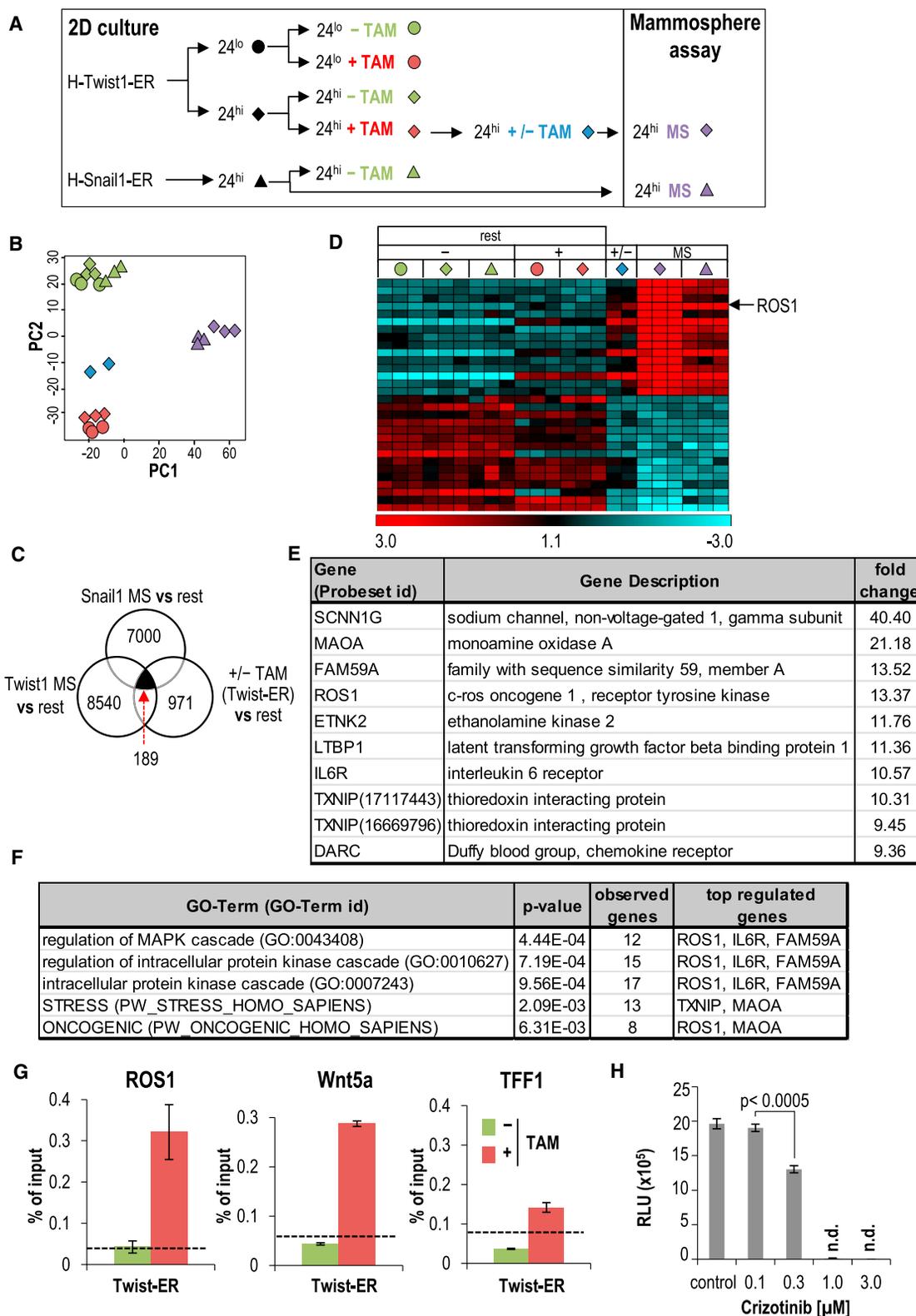
Figure 4. Transient Twist1 Activation Permanently Alters Cell State

(A) Cells included in gene expression profiling: control (green), 15-day TAM (red), 15-day TAM followed by 9-day TAM withdrawal (blue), MS (purple), HMLE-Twist1-ER 24^{lo} (circle), and 24^{hi} (rhomb), HMLE-Snail1-ER 24^{hi} (triangle).

(legend continued on next page)

to these observations, targeting mesenchymal cells might in some instances promote, rather than inhibit, proliferation both in the primary tumor and at metastatic sites.

These observations are in line with recent studies using mouse models of breast and squamous cell tumorigenesis to demonstrate that Snail1 or Twist1 deactivation is necessary for metastatic outgrowth (Tran et al., 2014; Tsai et al., 2012). Similarly, EMT was previously shown to inhibit rather than promote stem-cell-like traits in a number of experimental systems (Celià-Terrassa et al., 2012; Korpal et al., 2011; Sarrio et al., 2012). Finally, some EMT-TFs, such as Prrx1, promote mesenchymal differentiation and invasion, but not tumorigenicity (Ocaña et al., 2012). In support of these experimental data, we did not observe an overt loss of E-cadherin expression in serial sections of samples taken from the invasive front of 126 high-grade ductal carcinomas (Figure S4E; Table S1), consistent with recent observations that complete mesenchymal transdifferentiation is not required for Twist1 to induce invasion (Shamir et al., 2014).

We contribute an integrative mechanism of EMT-TF action to the contradictory observation that EMT is associated both with induction and inhibition of stem-cell-like traits because these can arise as stable traits after Twist1 or Snail1 deactivation. We hypothesize that the resultant altered epithelial cell state might promote metastatic outgrowth. Indeed, this priming mechanism adds to the increasing number of oncogenic functions of EMT-TFs not linked to EMT directly (Puisieux et al., 2014).

Our observations suggest that transient Twist1 or Snail1 activation may leave a tractable epigenetic footprint, a plausible scenario, since these master regulators are capable of recruiting chromatin modifiers (Bedi et al., 2014). Within a gene expression signature characteristic for this altered epithelial cell state, we identified the orphan receptor tyrosine kinase ROS1 as a potential drug target. Future studies might yield diagnostic tools to determine whether tumor cells have experienced EMT-TF activity in the past and develop strategies to target metastatic outgrowth.

EXPERIMENTAL PROCEDURES

Migration Assay

Cells (2.5×10^4) were seeded into 24-well culture inserts with 8 μm pores (BD Falcon). After 24 hr, nonmigrated cells were removed from the upper side of the insert with a cotton swab, and cells on lower insert surface were fixed and stained with the Hemacolor Rapid staining Set (Merck). All migrated cells per insert were counted. Data are presented as migrated cells per insert. Experiments were performed in triplicates.

MS Assay

The assay was performed as previously described with modifications (Dontu et al., 2003). One hundred cells or less were seeded per well in 96-well ultra-low-adhesion plates (Corning) in Dulbecco's modified Eagle's medium/F12 medium (Life Technologies) containing 1.0% methylcellulose (R&D Systems) supplemented with 5 ng/ml epidermal growth factor (Millipore), 20 ng/ml basic fibroblast growth factor (Millipore), 0.5 μg/ml hydrocortisone (Sigma), 10 μg/ml insulin (Sigma), 4 μg/ml heparin (Sigma), and 1× B27 (Life Technologies). For serial passaging, spheres were dissociated into single cells by trypsinization and replated.

3D Collagen Cultures

For 3D embedded cultures, gels containing 1.3 mg/ml collagen (BD Biosciences) and 0.1 M HEPES were mixed with cells in mammary epithelial cell growth medium, poured in 6- or 24-well plates and allowed to solidify prior feeding. Carmine and immunostaining of gels was done according to standard protocols, and gels were analyzed using either a standard light microscope or a laser scanning confocal microscope (Olympus). To measure proliferation in 3D collagen cultures, gels were digested with collagenase I followed by trypsinization to obtain a single-cell suspension. The number of cell doublings (n) was calculated as follows: 2^n = (number of cells at endpoint/number of initially seeded cells).

Statistical Analysis

Data are presented as mean ± SEM. A Student's test (two-tailed) was used to compare two groups ($p < 0.05$ was considered significant) unless otherwise indicated.

ACCESSION NUMBERS

The GEO accession number for the array data reported in this paper is GSE61206.

SUPPLEMENTAL INFORMATION

Supplemental Information includes Supplemental Experimental Procedures, four figures, one table, and two movies and can be found with this article online at http://dx.doi.org/10.1016/j.celrep.2014.12.032.

AUTHOR CONTRIBUTIONS

J.M.S., E.P., and C.H.S. designed and analyzed experiments and wrote the manuscript. J.M.S. and E.P. performed experiments, C.H.S. conceptualized the study. M.I. and J.B. performed and analyzed microarrays. H.S.B., S.K., and K.S. provided clinical samples and data. V.K. and S.A.J. performed chromatin immunoprecipitation analysis. J.R.L. developed the 3D collagen assay. D.D., B.H., and U.J.K. performed confocal microscopy. S.S. and F.T. provided bioinformatic support.

(B) Principal component analysis following unsupervised clustering of samples described in (A).

(C) Venn diagram: differentially expressed genes regulated in Snail1-MS, Twist1-MS, or 2D-cultured cells after transient Twist1 activation. The 189-gene signature represents the overlap of differentially regulated genes shared by these groups.

(D) Heatmap: top 15 upregulated and downregulated expression values of the 189-gene signature as described in (C). Red (high) and blue (low) indicates log2 expression values. Scale bar is in log2. The legend is as in (A).

(E) Top 10 upregulated genes of the 189 gene signature with corresponding fold change in Twist1-MS versus rest comparison (B).

(F) GO-term analyses: significantly enriched terms containing top-10 upregulated genes (E).

(G) Chromatin Immunoprecipitation: HMLE-Twist1-ER 24[hi] control (−) and 15-day TAM (+). TFF1 gene as negative control. Data indicate percentage (%) of input. Dotted line indicates IgG background (n = 3).

(H) MS assay: fourth generation of MS derived from 24^{hi} cells. Crizotinib was added daily at indicated concentrations. control, untreated MS; n.d., not detectable. Cell number quantified with Cell-Titer Glo.

Data are presented as mean ± SEM. See also Figures S4.

REFERENCES

Ansieau, S. (2013). EMT in breast cancer stem cell generation. Cancer Lett. *338*, 63–68.

Bedi, U., Mishra, V.K., Wasilewski, D., Scheel, C., and Johnsen, S.A. (2014). Epigenetic plasticity: a central regulator of epithelial-to-mesenchymal transition in cancer. Oncotarget *5*, 2016–2029.

Bergethon, K., Shaw, A.T., Ou, S.-H.I., Katayama, R., Lovly, C.M., McDonald, N.T., Massion, P.P., Siwak-Tapp, C., Gonzalez, A., Fang, R., et al. (2012). ROS1 rearrangements define a unique molecular class of lung cancers. J. Clin. Oncol. *30*, 863–870.

Casas, E., Kim, J., Bendesky, A., Ohno-Machado, L., Wolfe, C.J., and Yang, J. (2011). Snail2 is an essential mediator of Twist1-induced epithelial mesenchymal transition and metastasis. Cancer Res. *71*, 245–254.

Celià-Terrassa, T., Meca-Cortés, O., Mateo, F., de Paz, A.M., Rubio, N., Arnal-Estapé, A., Ell, B.J., Bermudo, R., Díaz, A., Guerra-Rebollo, M., et al. (2012). Epithelial-mesenchymal transition can suppress major attributes of human epithelial tumor-initiating cells. J. Clin. Invest. *122*, 1849–1868.

Chaffer, C.L., Brennan, J.P., Slavin, J.L., Blick, T., Thompson, E.W., and Williams, E.D. (2006). Mesenchymal-to-epithelial transition facilitates bladder cancer metastasis: role of fibroblast growth factor receptor-2. Cancer Res. *66*, 11271–11278.

Dontu, G., Abdallah, W.M., Foley, J.M., Jackson, K.W., Clarke, M.F., Kawamura, M.J., and Wicha, M.S. (2003). In vitro propagation and transcriptional profiling of human mammary stem/progenitor cells. Genes Dev. *17*, 1253–1270.

Elenbaas, B., Spirio, L., Koerner, F., Fleming, M.D., Zimonjic, D.B., Donaher, J.L., Popescu, N.C., Hahn, W.C., and Weinberg, R.A. (2001). Human breast cancer cells generated by oncogenic transformation of primary mammary epithelial cells. Genes Dev. *15*, 50–65.

Frisch, S.M., and Francis, H. (1994). Disruption of epithelial cell-matrix interactions induces apoptosis. J. Cell Biol. *124*, 619–626.

Gupta, P.B., Onder, T.T., Jiang, G., Tao, K., Kuperwasser, C., Weinberg, R.A., and Lander, E.S. (2009). Identification of selective inhibitors of cancer stem cells by high-throughput screening. Cell *138*, 645–659.

Korpal, M., Ell, B.J., Buffa, F.M., Ibrahim, T., Blanco, M.A., Celià-Terrassa, T., Mercatali, L., Khan, Z., Goodarzi, H., Hua, Y., et al. (2011). Direct targeting of Sec23a by miR-200s influences cancer cell secretome and promotes metastatic colonization. Nat. Med. *17*, 1101–1108.

Kowalski, P.J., Rubin, M.A., and Kleer, C.G. (2003). E-cadherin expression in primary carcinomas of the breast and its distant metastases. Breast Cancer Res. *5*, R217–R222.

Lamouille, S., Xu, J., and Derynck, R. (2014). Molecular mechanisms of epithelial-mesenchymal transition. Nat. Rev. Mol. Cell Biol. *15*, 178–196.

Lim, J., and Thiery, J.P. (2012). Epithelial-mesenchymal transitions: insights from development. Development *139*, 3471–3486.

Mani, S.A., Guo, W., Liao, M.-J., Eaton, E.N., Ayyanan, A., Zhou, A.Y., Brooks, M., Reinhard, F., Zhang, C.C., Shipitsin, M., et al. (2008). The epithelial-mesenchymal transition generates cells with properties of stem cells. Cell *133*, 704–715.

Morel, A.-P., Lièvre, M., Thomas, C., Hinkal, G., Ansieau, S., and Puisieux, A. (2008). Generation of breast cancer stem cells through epithelial-mesenchymal transition. PLoS ONE *3*, e2888.

Nieto, M.A. (2011). The ins and outs of the epithelial to mesenchymal transition in health and disease. Annu. Rev. Cell Dev. Biol. *27*, 347–376.

Ocaña, O.H., Córcoles, R., Fabra, A., Moreno-Bueno, G., Acloque, H., Vega, S., Barrallo-Gimeno, A., Cano, A., and Nieto, M.A. (2012). Metastatic colonization requires the repression of the epithelial-mesenchymal transition inducer Prrx1. Cancer Cell *22*, 709–724.

Puisieux, A., Brabletz, T., and Caramel, J. (2014). Oncogenic roles of EMT-inducing transcription factors. Nat. Cell Biol. *16*, 488–494.

Rossi, A., Maione, P., Sacco, P.C., Sgambato, A., Casaluce, F., Ferrara, M.L., Palazzolo, G., Ciardiello, F., and Gridelli, C. (2014). ALK inhibitors and advanced non-small cell lung cancer (review). Int. J. Oncol. *45*, 499–508.

Sarrio, D., Franklin, C.K., Mackay, A., Reis-Filho, J.S., and Isacke, C.M. (2012). Epithelial and mesenchymal subpopulations within normal basal breast cell lines exhibit distinct stem cell/progenitor properties. Stem Cells *30*, 292–303.

Scheel, C., and Weinberg, R.A. (2012). Cancer stem cells and epithelial-mesenchymal transition: concepts and molecular links. Semin. Cancer Biol. *22*, 396–403.

Scheel, C., Eaton, E.N., Li, S.H.-J., Chaffer, C.L., Reinhardt, F., Kah, K.-J., Bell, G., Guo, W., Rubin, J., Richardson, A.L., and Weinberg, R.A. (2011). Paracrine and autocrine signals induce and maintain mesenchymal and stem cell states in the breast. Cell *145*, 926–940.

Shamir, E.R., Pappalardo, E., Jorgens, D.M., Coutinho, K., Tsai, W.-T., Aziz, K., Auer, M., Tran, P.T., Bader, J.S., and Ewald, A.J. (2014). Twist1-induced dissemination preserves epithelial identity and requires E-cadherin. J. Cell Biol. *204*, 839–856.

Shi, J., Wang, Y., Zeng, L., Wu, Y., Deng, J., Zhang, Q., Lin, Y., Li, J., Kang, T., Tao, M., et al. (2014). Disrupting the interaction of BRD4 with diacetylated Twist suppresses tumorigenesis in basal-like breast cancer. Cancer Cell *25*, 210–225.

Stankic, M., Pavlovic, S., Chin, Y., Brogi, E., Padua, D., Norton, L., Massagué, J., and Benezra, R. (2013). TGF-β-Id1 signaling opposes Twist1 and promotes metastatic colonization via a mesenchymal-to-epithelial transition. Cell Rep. *5*, 1228–1242.

Tam, W.L., Lu, H., Buikhuisen, J., Soh, B.S., Lim, E., Reinhardt, F., Wu, Z.J., Krall, J.A., Bierie, B., Guo, W., et al. (2013). Protein kinase C α is a central signaling node and therapeutic target for breast cancer stem cells. Cancer Cell *24*, 347–364.

Tran, H.D., Luitel, K., Kim, M., Zhang, K., Longmore, G.D., and Tran, D.D. (2014). Transient SNAIL1 expression is necessary for metastatic competence in breast cancer. Cancer Res. *74*, 6330–6340.

Tsai, J.H., Donaher, J.L., Murphy, D.A., Chau, S., and Yang, J. (2012). Spatiotemporal regulation of epithelial-mesenchymal transition is essential for squamous cell carcinoma metastasis. Cancer Cell *22*, 725–736.